Journal of the European Ceramic Society **17** (1997) 1193–1200

PII: S0955-2219(96)00229-4
0955-2219/97/$17.00

Quantification of the Internal Structure in Ceramic Green Bodies using Computer-Assisted Optical Imaging

Nozomu Uchida[a] and Lennart Bergström[b]*

[a]Department of Chemistry, Nagaoka University of Technology, Kamitomioka, Nagaoka 940-21, Japan
[b]Institute for Surface Chemistry, Box 5607, S-114 86 Stockholm, Sweden

(Received 9 July 1996; revised version received 4 November 1996; accepted 11 November 1996)

Abstract

The internal structure of ceramic green bodies has been characterised by combining a computer-controlled optical microscope with an image analysing system to provide statistically reliable data of the pore size distribution. The calcined porous alumina ceramic green body was made transparent by utilising the immersion liquid technique which enabled the interior of the body to be observed. It was demonstrated how internal defects such as pores could be detected using this technique and an automated sequence of obtaining internal structure images and transferring and processing them using an image analysing software system has been developed. The technique proved to be a simple and rapid method of accurately determining the number distribution of pores in an alumina green body. © 1997 Elsevier Science Limited.

1 Introduction

It is well known that the fracture strength of ceramics is governed by the size of defects or flaws i.e. pores, inclusions, agglomerates, cracks and other types of inhomogeneities, which can act as the fracture origins as described by the Griffith equation,[1]

$$\sigma = \frac{YK_{IC}}{\sqrt{C}} \quad (1)$$

where σ is the fracture stress, K_{IC} the fracture toughness, C the defect size and Y is a factor that depends on the position and shape of the defect. Most of these defects are originally introduced into the green body during the powder processing steps, i.e. powder production, dispersion and consolidation of powders, and remain as strength-limiting flaws in the sintered material.[2,3] Hence, in order to improve the mechanical performance and the reliability of ceramics, the size and concentration of the defects in the green body must be minimised by optimising the processes prior to sintering.[4–7] The defects which govern the fracture strength of brittle ceramics are typically in the size range 10–100 μm where the larger defects can occur in very low number densities.

Many approaches, including the colloidal processing route, have been taken to achieve the goal of defect minimisation and have sometimes led to significant improvements of the reliability of the ceramic material.[8] The common method of verifying improved processing and reliability is mechanical testing of sintered pieces together with fractography identification of fracture origins. This destructive method, which needs a lot of samples to give a statistically acceptable result, is usually too costly and time-consuming to allow extensive testing and optimisation.

Other techniques, such as mercury porosimetry or SEM observation of polished surfaces, can also be used for defect characterisation of both sintered and unfired, consolidated materials. However, it is difficult for these conventional characterisation techniques to identify and quantify defects at very low number densities. Although new techniques, such as X-ray tomography, ultrasonics and NMR imaging have been proposed, these methods usually suffers from lack of resolution and very costly equipment.[9–12] The epoxy impregnation/sectioning technique can provide quasi-three-dimensional information; however, the sample preparation is time-consuming.[13]

Recently, it was demonstrated how a new and powerful method, called the immersion liquid technique, can be used to observe the internal structure of ceramic green or calcined bodies.[14,15] In this technique, porous ceramic bodies are made transparent by filling the pores with a liquid which

*To whom correspondence should be addressed.

has a refractive index close to that of the ceramic material. The internal structure of the immersion-liquid-filled ceramic body, including the defects, can then be observed by an ordinary optical microscope. This method has been applied to a number of different systems including spray-dried alumina,[14] silicon nitride,[16] and zirconia,[17] and in a study of the effect of forming pressure on the internal structure of alumina green bodies.[18] Since the sample preparation procedure for the immersion liquid technique is very simple and optical microscopes are available at relatively low cost, this method has the potential for being very useful in the characterisation of internal structure and identification of defects in ceramic green bodies and spray dried granules.

In this study we will show how the liquid immersion technique can be used in a standardised way as a simple and accurate method of identifying and quantifying the size and number frequency of pores in a ceramic green body. Relatively large volumes of calcined ceramic green bodies have been examined by combining a computer-controlled optical microscope with an image analysing system to provide statistically reliable data. The paper describes how the design of the automatic procedure was developed, and the feasibility of the method is illustrated on a system containing artificially introduced pores.

2 Experimental

2.1 Experimental system

A model system consisting of an alumina calcined body containing artificially introduced uniform pores has been used. The alumina powder (UA-5105, Showa Denko, Japan) having a mean particle diameter, d, of 0·25 μm and a specific surface area of 10 m^2/g, was mixed with organic polystyrene spheres suspended in aqueous medium (Particle-Size Standards, $d = 39{\cdot}8 \pm 0{\cdot}6$ μm, Duke Scientific Corp., USA). The number concentration of the polystyrene spheres in the alumina-polystyrene mixture, the standard sample, was approximately 20 spheres per gram powder. After drying the alumina-bead mixture in a oven at 60°C overnight, the mixture was ground lightly and uniaxially pressed at 100 MPa into a pellet of cylindrical shape ($\varnothing$ = 12·5 mm, thickness $\approx$ 1·5 mm). The pressed pellets were calcined at 1100°C for 1 h to give proper mechanical strength against the subsequent treatment and to burn out the polymer beads. The calcined pellet was polished with grinding paper to a thickness of approximately 1 mm. The thickness was determined using a micrometer. The relative density of the calcined green body was estimated to be 53% TD (theoretical density) from the dimension (volume) and weight. A blank sample (without organic polymer beads) was also prepared from the alumina powder following the pressing and sintering procedure above.

The porous, calcined ceramic green body was made transparent by using diiodomethane; CH_2I_2 (synthesis grade, Merck) as the immersion liquid. The calcined specimen was placed on an observation glass and diiodomethane was placed around the sample. Penetration of the liquid was facilitated by removing the air in the sample using a water aspirator for 10 min. A cover glass was put onto the saturated ceramic green body before optical micrographs were taken in order to suppress evaporation of the immersion liquid and to keep the surface of the green body flat. With the present system it was possible to use the covered sample for 24 h without any significant evaporation occurring.

2.2 Image analysing system

The optical image analysis system consists of an optical microscope (Axioplan, Zeiss) and image analysing software (MicroGOP2000/S, CONTEXTVISION) installed on a engineering work station; EWS (SPARC Classic, Sun Microsystems). The schematic system constitution is shown in Fig. 1. An X-Y-Z table (Scanning Stage Control and Auto focusing Unit, SSC03, Iduna) which can be controlled from the EWS is mounted on the microscope. Microscope images are captured by a CCD camera (CCD72, MTI) and transmitted to the EWS.

3 Results and Discussion

The interior of porous ceramic green bodies may be observed and characterised by optical

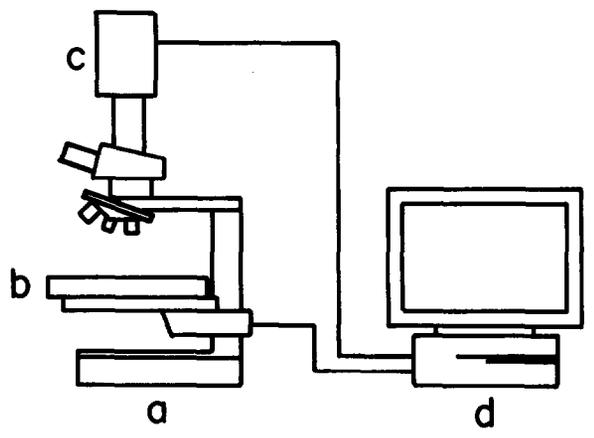

Fig. 1. Schematic outline of the image analysing system. (a) Microscope, (b) XYZ table, (c) CCD camera and (d) engineering work station.

microscopy only if light scattering is substantially reduced. This can be achieved using the immersion liquid technique since scattering of light does not occur at the interface between a solid particle and a medium if the refractive index difference (n_{solid}–n_{liquid}) is sufficiently small.[19] Hence, when the pore volume in a ceramic green or calcined body is filled with an immersion liquid, which has a refractive index close to that of the ceramic material, the internal light scattering is reduced and the body becomes (nearly) transparent. Although a very close index matching makes it possible to characterise relatively thick samples, a minimum contrast, i.e. light scattering, is needed to enable identification of pores in the green body. The contrast in the optical micrographs becomes particularly important when an automated image analysis sequence is to be developed. Hence, there is an optimum of the index matching and the sample thickness which has to be found for each system. Earlier studies have shown that diiodomethane (n = 1·74) and 2-bromonaphthalene (n = 1·64) can be used to make alumina (n = 1·76) green bodies transparent.[15,18] For ceramic materials with higher refractive indices, e.g. zirconia (n = 2·15) and silicon nitride (n = 1·96),[20] the refractive index of the immersion liquid can be increased by adding sulphur and phosphorus to diiodomethane.[16,17]

Recently, the immersion liquid technique was quantitatively evaluated by measuring the size and amount of artificially introduced pores in alumina green bodies.[21] Mixing the powder with polymer micro spheres of different sizes, ranging from 5 to 40 μm, resulted in artificially introduced pores which could be easily detected due to the spherical shape. It was found that by an appropriate choice of sample thickness and refractive index of the immersion liquid, it was possible to accurately determine the size and number density of the artificially introduced pores. In this study, we employed a similar approach by mixing polystyrene spheres of $d \approx 40$ μm with the fine alumina powder, forming a ceramic green body which was calcined and prefired at 1100°C. Figure 2 shows the optical micrographs of the interior of the standard and blank alumina samples. The circles of a diameter around 40 μm dispersed on the images of Figs 2(a) and (b) are the artificially introduced pores stemming from the polymer micro-spheres. Due to the random pore distribution and limited focal depth, some of the pores are in focus (marked with f) while others are slightly out of focus (marked with o). The size of the pores is expected to be closely correlated to the size of the polymer micro-spheres since previous work has shown negligible changes in pore size distribution during calcination and prefiring.[21]

Figure 2 illustrates that diiodomethane is an excellent immersion liquid for alumina since images from the interior can be obtained while a sufficient contrast between pores and matrix (particles) is retained. Previous work showed that a thickness of 1 mm was the maximum thickness for quantitative analysis using diiodomethane as immersion liquid,[21] hence, all calcined green bodies were ground to a thickness not exceeding this value. The black spots which can be found in all the micrographs (Figs 2(a)–(c)), hence in both the standard and blank samples, originate from objects which have a significantly different refractive index compared to the immersion liquid. Possible sources are inclusions or other contaminations which have remained during calcination, or pores which have not been filled with the immersion liquid.

Figure 3 shows the binary images obtained by image analysis of the optical, 'raw' micrographs. By comparing the binary image (Fig. 3(a)) and the optical micrograph (Fig. 2(a)) of the same object, it is found that pores which are out of focus in the optical micrograph are not transferred to the binary image. This effect is a result of the current definition of the edge detection which was set to minimise the possibility of introducing artefacts. This means that only the edge of the equatorial diameter of the spherical pores is transferred to the binary image. If the focal plane exists above or below the equator plane, the contrast between the pore and the matrix is not sharp enough. Hence, the risk of detecting pores of varying sizes due to the position in the focal plane is minimised.

This study has focused on identification of objects in the size range from 15 μm to 100 μm which corresponds to the defect size range controlling the strength of most ceramic materials available today. To maximise the information in each image, a relatively low magnification of the optical microscope (5 × 10 times) was chosen. The large number density of small (< 10 μm) defects and the poor resolution in this size range, precluded the design of an image processing sequence over the entire pore size range without introducing artefacts in the low size range. Hence, objects smaller than 15 μm were excluded from the binary images. If smaller objects are to be classified, a larger magnification and thus a smaller displayed area and a more shallow focal depth has to be used. No attempt to increase the resolution was made but it is clear that the image sampling program has to be tailored for the magnification being used.

Since the positioning of the sample, as well as obtaining and analysing optical images, can be computer-controlled, it was possible to develop a fully automated sequence for characterising the

frequency and size of pores in a well-defined sample volume by scanning the transparent porous ceramic body. The scanning sequence is shown schematically in Fig. 4. The automated sequence created on the MicroGOP 2000/S consists of the following steps:

(i) The absolute position of the first image is determined by identifying the upper and lower surface of the sample and using the calibrated X-Y-Z-table to reach a suitable starting position. At this starting position (fixed X-Y position) the Z position is varied in predefined steps.

(ii) During the Z direction scan, raw images (optical micrograph) are obtained at every 80 μm as shown in Fig. 4(a). The distance between the Z images was selected so that all of the artificially introduced pores will be identified. With the use of a more shallow

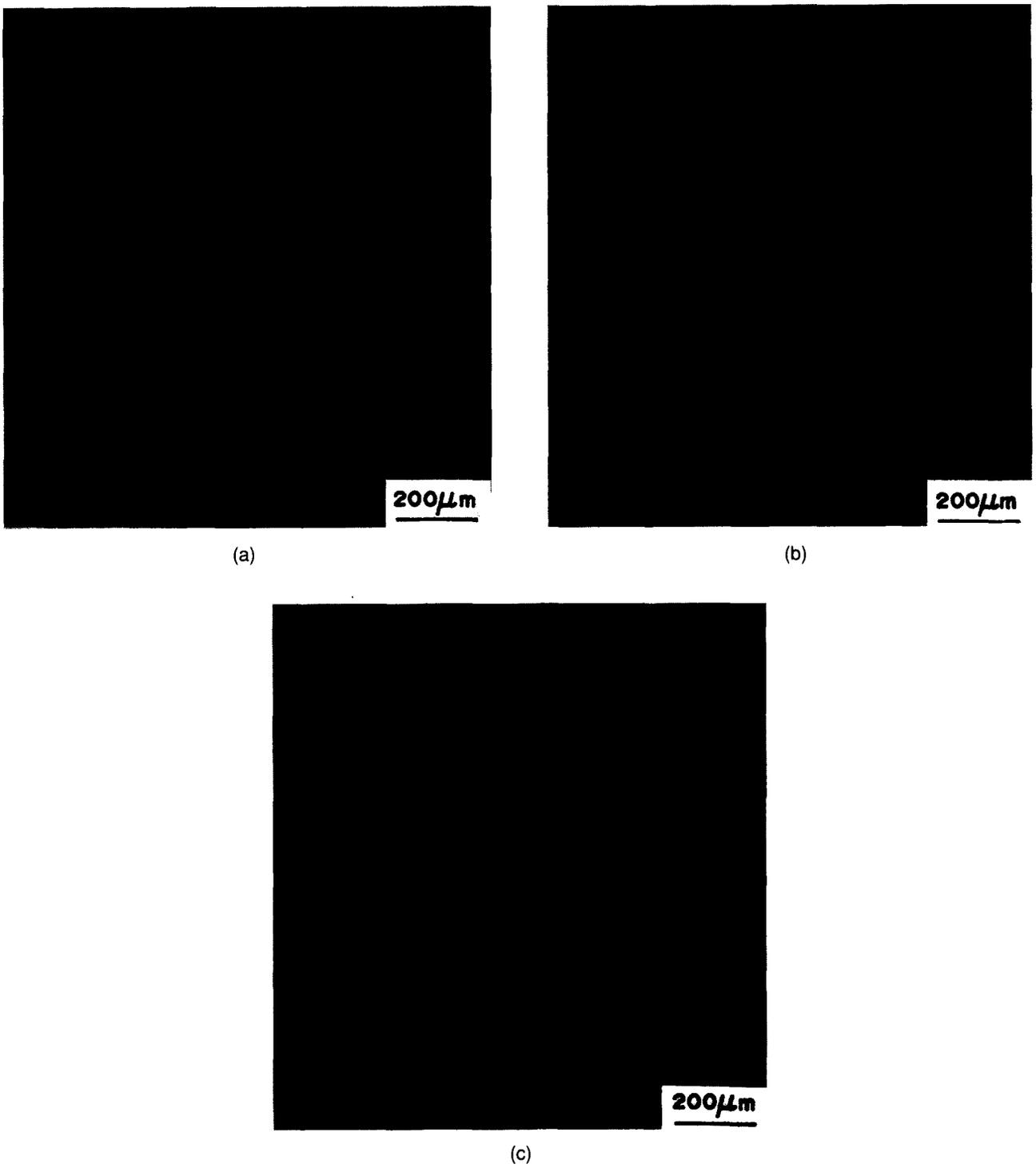

Fig. 2. Optical micrographs of the internal structure of calcined alumina green bodies using diiodomethane as immersion liquid. Figs 2(a) and (b) are images, with a size of 1180 × 1180 μm, of the standard sample at identical X-Y position but varying Z position, at 160 μm and 320 μm from the bottom, respectively. Some of the spherical pores are marked with an arrow, f: pores in focus, and o: pores slightly out of focus. Figure 2(c) represents the interior image of the blank alumina sample.

focal depth (higher magnification), the Z image distance has to be reduced significantly.

(iii) Each optical image is processed to detect edges, i.e. the boundaries between the objects such as defects and the matrix, and to enhance contrast and then transformed to the binary (monochrome) image in which the objects and the matrix are distinguished clearly.

(iv) The obtained binary images, at a fixed X-Y position and variable Z position, are superimposed into one binary image to give an integrated image, the so-called penetrative image.

(v) The maximum diameter of each object in the penetrative image is measured and stored in the common data file. Then the X and/or Y position is changed (X-Y scan as seen in Fig. 4(b)) and the above treatment from (ii) is repeated.

(vi) After a pre-defined number of penetrative images have been created, a pore size distribution diagram of pore size versus pore number frequency per unit volume is obtained by normalising to the examined volume.

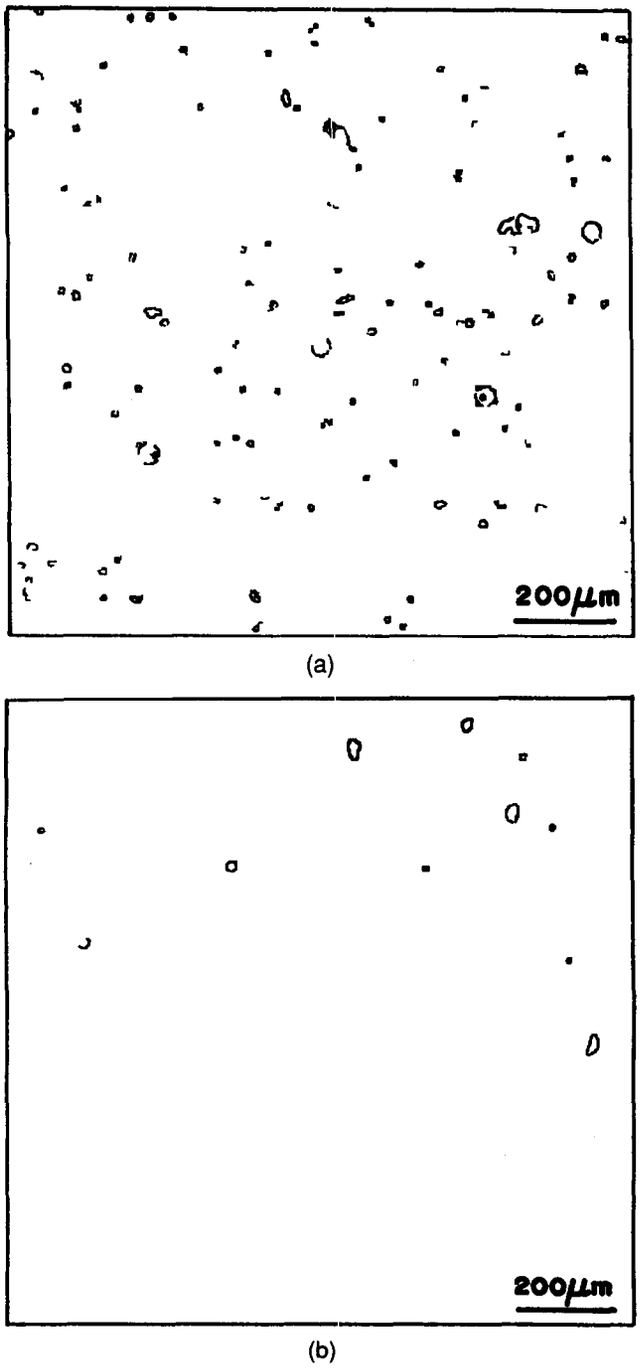

Fig. 3. Computer-processed binary images based on the optical images in; (a) Fig. 2(a), and (b) Fig. 2(c).

The penetrative images shown in Fig. 5 give a clear picture of the distribution of the larger pores in both the standard and blank samples. The binary images in Figs 3(a) and (b) are one of the 11 superimposed images in each of the penetrative images. The rough circles of a diameter around 40–60 μm in Fig. 5(a) are the artificially introduced pores. These types of pores can be easily distinguished, due to their spherical shape, from the other types of defects also present in the blank sample. The corresponding circles (pores) can also be found in Fig. 3(a). The larger concentration of smaller, irregular pores in the standard sample compared to the blank sample can be referred to differences in the sample preparation step. Hence, Fig. 5 illustrates how image analysis of optical micrographs of the interior of ceramic

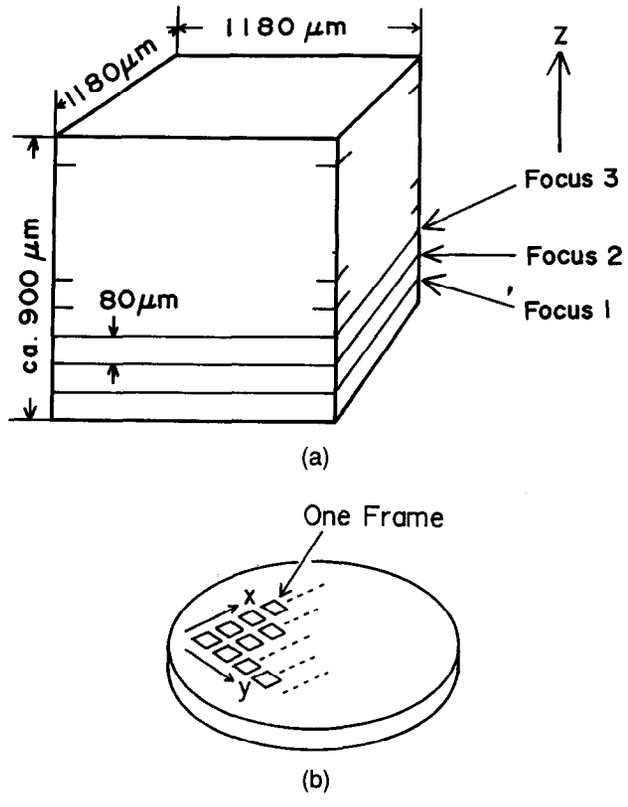

Fig. 4. Automated image collecting scheme. Images are collected by scanning in the Z direction (a) and in the X and/or Y direction (b).

green bodies using the immersion liquid technique can be used as a powerful method to identify defects and pores.

A relatively large sample volume was examined by changing the X and Y positions of the sample using the computer-controlled positioning table (See Fig. 4), and creating a penetrative image at each, predetermined X-Y position. In the current study, 12 different X-Y positions were examined at 11 different Z positions, hence a total of 132 images were obtained and image analysed for each sample. With the magnification being used, this set of analysed images corresponds to examined volumes of approximately 15 mm^3 (number of penetrative images × area of image × thickness of sample). It took about 100 min to process 132 images using this image analysing system. The scanning and analysis was done in a fully automated manner.

Figures 6(a) and (b) show the defect size number distribution histograms for the standard and blank samples, respectively. The histograms are generated by sampling the identified objects from the 12 penetrative images in different classes and normalising the number to the investigated volume. The total numbers of collected objects in the size range 15–100 μm were 6186 in 15·06 mm^3, and 1289 in 15·53 mm^3, for the standard and blank samples, respectively. Both of the samples displayed a large concentration of pores in the size range 15–30 μm with the standard sample showing a significantly higher concentration. These pores correspond to the defects introduced in the powder processing and dry pressing step. The higher concentration of these small defects in the standard sample can probably be referred to poorer mixing compared to the blank sample.

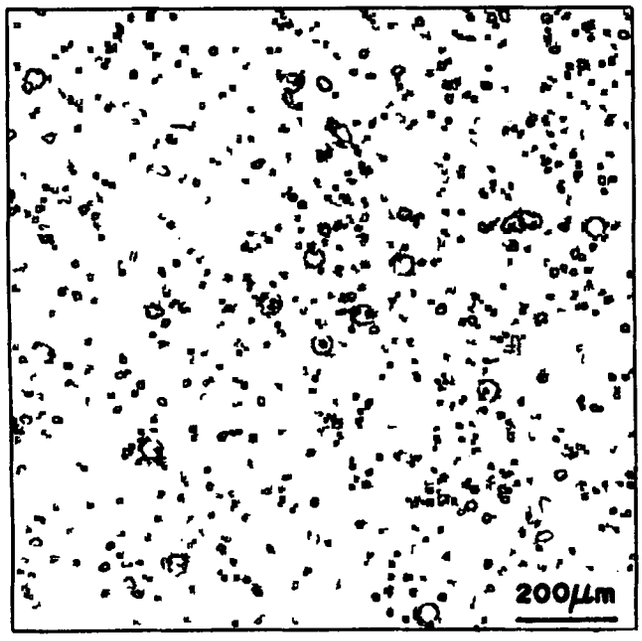

(a)

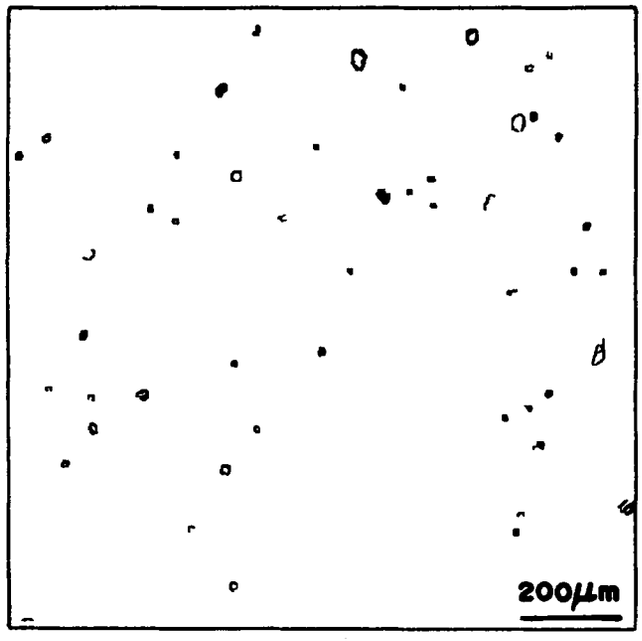

(b)

Fig. 5. Penetrative images from 11 superimposed micrographs at a fixed X-Y position representing an area of 1180 × 1180 μm and a thickness of approximately 900 μm for (a) standard sample and (b) blank sample.

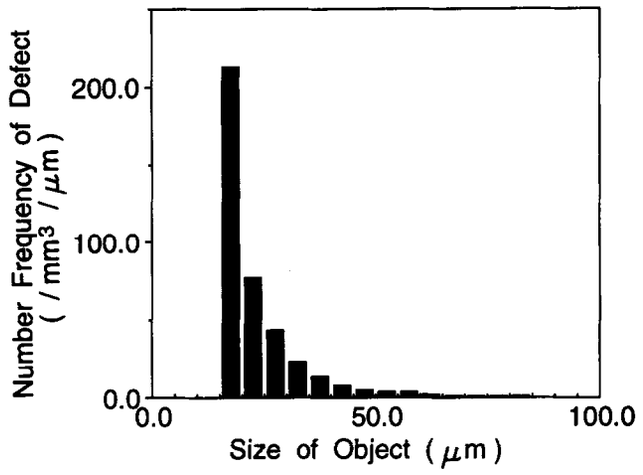

(a)

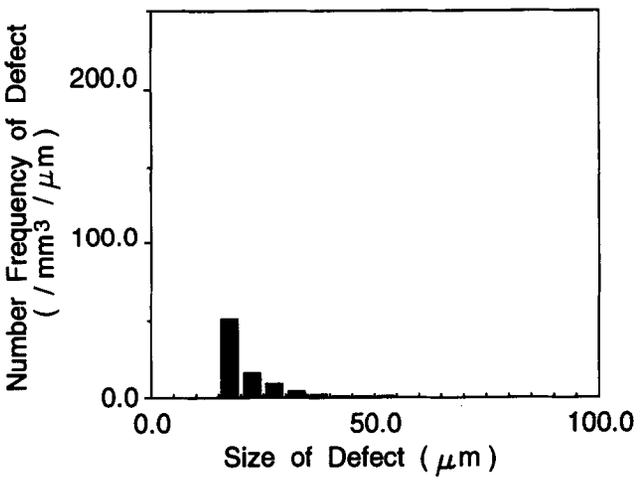

(b)

Fig. 6. Pore size distribution histograms per unit volume for (a) standard sample and (b) blank sample.

It should be noted that the number concentration of the smaller objects does not represent an absolute concentration since sufficiently small objects may be undetected with the current Z image step of 80 μm.

The standard sample (Fig. 6(a)) displays a significantly higher concentration of pores in the larger size range, 45–60 μm. Initially, we had expected that the pore distribution should be bimodal in the standard sample containing the artificially introduced pores, since the blank sample essentially does not exhibit any pores larger than 40 μm. Unfortunately, the higher defect population in the standard sample obscures such a simple identification but a comparison with Fig. 5(a) shows that the large majority of the pores in the larger pore size range have a spherical shape, indicating that these pores correspond mainly to the artificially introduced pores. A precise assignment of the large pores is complicated due to the difference in processing defect concentration between the standard and blank sample, making a normalisation of the artificial and processing pore concentration difficult. Surprisingly, the number concentration of identified objects in the size range 46–60 μm: 11·9 pores/mm^3 in the standard sample, corresponds rather well to the actual number concentration of introduced polystyrene spheres: estimated to $\approx$11 spheres/mm^3 in the green body. However, at present, this correlation can only be taken as an indication of the quantification potential of the computer-assisted optical imaging method. More data from samples where the pore origin can be unequivocally assigned have to be analysed before any statistical accuracy of the present method can be defined.

There are two main reasons why the size of the pores increases in the computer-generated binary images compared to the original micrographs. First, the edge detecting function in the image analysing system is the key parameter when a binary image is created from a micrograph. This function traces the edge of the object with a finite resolution which tends to enhance the size of the identified objects. Secondly, although objects smaller than 15 μm are ignored when the binary image is being constructed, they might interfere with the edge detection of larger objects. With the current image analysis program, these two effects may cause the pore size to increase up to 130% of the original size. It is possible that more sophisticated image analysis techniques, e.g. the sparse Hough transformation which can recognise separate objects within an aggregate,[22] could remedy some of the shortcomings of the present method.

Strictly speaking, the method described in this article is a quasi-three-dimensional analysis technique since the method is based on superposition and integration of two-dimensional segments (images) with the normal direction along the Z axis. A full three-dimensional analysis method would require that images are sampled from all directions and then processed using some type of 3-D tomography software. If the two-dimensional segments contain all the required information, i.e. images of all the pores, the present method should yield a satisfactory representation of the concentration of interior defects. However, if some information is lost, e.g. due to a too large stepping distance in the Z direction, the choice of the normal direction may be crucial. This effect will be pronounced in materials having an anisotropic microstructure where the mechanical strength also might vary significantly depending on the loading direction. Since the present prefired material has an isotropic microstructure, consisting of fine, equiaxed alumina grains with the artificially introduced pores well dispersed in the matrix, such effects are expected to be of minor importance.

This study shows how image analysed binary images and a generated pore size distribution diagram can give important information regarding the internal structure of ceramic green bodies. From the penetrative binary images the nature and possible origin of the defects can be estimated. The pore size distribution diagram results in statistical information which can be used for estimations of fracture strength and Weibull parameter on the basis of classical fracture mechanics of brittle materials. We believe that the fully automated method presented is an attractive alternative to the much more time-consuming sampling of fracture strength of many specimens.[23] The processing time of a set volume of a ceramic green body depends on a number of factors; e.g. the magnification being used (image area and focal depth), the lower cut-off range of the defect size being characterised, the required statistical reliability and the capability and speed of the MPU of the EWS. A high magnification and a high statistical reliability obviously require a large number of images to be analysed.

5 Summary and Conclusions

A systematic characterisation procedure for the internal structure of porous ceramic bodies using computer-assisted optical imaging has been developed. It was shown how optical microscopy can yield representative images of the pores and other types of defects in ceramic green bodies by using the immersion liquid technique. A fully automated sequence for characterising the frequency and size

of pores was developed by using a computer-controlled optical microscope and an image analysis system. By optimising the edge detection sequence, it was possible to obtain binary images which are appropriate representations of the optical micrographs.

Using this procedure, relatively large volumes of porous ceramic bodies can be automatically examined and the size and concentration of defects such as pores and inclusions can be detected and quantified. The features of this novel technique were illustrated by characterising the pore concentration in an alumina green body containing artificially introduced pores with a size around 40 μm. It was found that the results from the optical imaging method corresponded semi-quantitatively to the estimation of the introduced pore concentration. It can be concluded that the method developed in this study is able of performing a simple, rapid and relatively accurate characterisation of the defect concentration in porous ceramic bodies. In fact, optical imaging is a sufficiently easy and swift technique to be considered as a technique suitable for routine characterisation of ceramic green bodies of simple shapes, and has the potential of being an indispensable tool for optimisation of ceramic processing.

Acknowledgements

Prof. Keizo Uematsu is gratefully acknowledged for introducing the authors to the immersion liquid technique and very fruitful discussions. This work was supported financially by the Swedish National Board for Industrial and Technical Development (NUTEK).

References

1. Griffith, A. A., *Phil. Trans. R. Soc. London*, 1920, **A221**, 163.
2. Roosen, A. and Bowen, H. K., Influence of various consolidation techniques on the green microstructure and sintering behavior of alumina powders. *J. Am. Ceram. Soc.*, 1988, **71**(11), 970–977.
3. Lange, F. F., Powder processing science and technology for increased reliability. *J. Am. Ceram. Soc.*, 1989, **72**, 3–15.
4. Aksay, I. A., Microstructure control through colloidal consolidation. In *Advances in Ceramics*, vol. 9, ed. J. A. Mangels and G. L. Messing. American Ceramic Society, Westerville, OH, 1984, pp. 94–104.
5. Pugh, R. J. and Bergström, L. (eds), *Surface and Colloid Chemistry in Advanced Ceramics Processing*. Marcel Dekker, New York, 1994.
6. Nies, C. W. and Messing, G. L., Effect of glass transition temperature of polyethylene glycol-plasticized polyvinyl alcohol on granule compaction. *J. Am. Ceram. Soc.*, 1984, **67**(4), 301–304.
7. Frey, R. G. and Halloran, J. W., Compaction behavior of spray-dried alumina. *J. Am. Ceram. Soc.*, 1984, **67**(3), 199–203.
8. Carlström, E., Defect minimisation in silicon carbide, silicon nitride and alumina ceramics. PhD thesis, Chalmers University of Technology, Göteborg, Sweden, 1989.
9. Ackerman, J. L., Garrido, L., Ellingson, W. A. and Wayand, D. J., The use of NMR imaging to measure porosity and binder distribution in green-state and partially sintered ceramics. In *Nondestructive Testing of High-Performance Ceramics*. American Ceramic Society, Columbus, OH, 1987, pp. 88–113.
10. Cobin, N. D., Pujari, V. K., Antal, J. J. and Marotta, A. S., A preliminary assessment of neutron radiography for detecting inhomogeneities in ceramics. In *Nondestructive Testing of High-Performance Ceramics*. American Ceramic Society, Columbus, OH, 1987, pp. 114–127.
11. Friedman, W. D., Harris, R. D., Engler, P., Hunt, P. K. and Srinivasan, M., Characterization of green ceramics with X-ray tomography and ultrasonics. In *Nondestructive Testing of High-Performance Ceramics*. American Ceramic Society, Columbus, OH, 1987, pp. 128–131.
12. Jones, M. P. and Blessing, G. V., Ultrasonic evaluation of spray-dried powder during and after compaction. In *Nondestructive Testing of High-Performance Ceramics*. American Ceramic Society, Columbus, OH, 1987, pp. 148–155.
13. Weeks, M. D. and Jaughner, J. W., Characterization of unfired ceramic microstructure. *Adv. Ceram.*, 1987, **21**, 793–800.
14. Uematsu, K., Kim, J.-Y., Kato, Z., Uchida, N. and Saito, K., Direct observation method for observing internal structure of ceramic green body. *Nippon Seramikkusu Kyoukai Gakujutsu Ronbunshi*, 1990, **98**(5), 515–516.
15. Uematsu, K., Kim, J.-Y, Miyashita, M., Uchida, N. and Saito, K., Direct observation of internal structure in spray-dried alumina granules. *J. Am. Ceram. Soc.*, 1990, **73**(8), 2555–2557.
16. Inoue, M., Kim, J.-Y., Kato, Z., Uchida, N., Uematsu, K. and Saito, K., Development of direct observation method for internal structure of spray-dried granule and green body of silicon nitride. In *Shin Sozai (New Materials)*. Japan MRS, Uchidaroukakuho, Tokyo, 1990, p. 59.
17. Kim, J.-Y., Inoue, M., Kato, Z., Uchida, N., Saito, K. and Uematsu, K., Direct observation of internal structure in spray-dried yttria-doped zirconia granule. *J. Mater. Sci.*, 1991, **26**, 2215–2218.
18. Uematsu, K., Miyashita, M., Kim, J.-Y., Kato, Z. and Uchida, N., Effect of forming pressure on the internal structure of alumina green bodies examined with immersion liquid technique. *J. Am. Ceram. Soc.*, 1991, **74**(9), 2170–2174.
19. Kingery, W. D., Bowen, H. J. and Uhlmann, D. R., In *Introduction to Ceramics*, 2nd edn, ch. 13. Wiley, New York, 1976, pp. 646–703.
20. Bergström, L., Meurk, A., Arwin, H. and Rowcliffe, D. J., Estimation of Hamaker constants from optical data using Lifshitz theory. *J. Am. Ceram. Soc.*, 1996, **79**(2), 339–348.
21. Ishikawa, H., Zhang, Y., Uchida, N. and Uematsu, K., Quantitative evaluation of immersion liquid technique. *J. Ceram. Soc. Jpn*, 1996, **104**(2), 133–136.
22. Kruis, F. E., van Denderen, J., Buurman, H. and Scarlett, B., Characterization of agglomerated and aggregated aerosol particles using image analysis, Part. Part. Syst. Charact. II, 1994, 426–435.
23. Kendall, K., Alford, N. McN. and Birchall, J. D., The strength of green bodies. In *Special Ceramics 8, British Ceramic Proceedings 37*, ed. S. P. Howlett and D. Taylor. Institute of Ceramics, Stoke-on-Trent, UK, 1986, pp. 255–265.